PHYSICAL REVIEW B **66**, 220101(R) (2002)

Self-interstitials in V and Mo

Seungwu Han,[1] Luis A. Zepeda-Ruiz,[1,2] Graeme J. Ackland,[4] Roberto Car,[1,3] and David J. Srolovitz[1,2]
[1]*Princeton Materials Institute, Princeton University, Princeton, New Jersey 08544*
[2]*Department of Mechanical and Aerospace Engineering, Princeton University, Princeton, New Jersey 08544*
[3]*Department of Chemistry, Princeton University, Princeton, New Jersey 08544*
[4]*Department of Physics and Astronomy, University of Edinburgh, Edinburgh EH9 3JZ, Scotland, United Kingdom*
(Received 22 October 2002; published 12 December 2002)

We report an extensive *ab initio* study of self-interstitials in V and Mo. Contrary to the widely accepted picture, the ⟨111⟩ dumbbell is found to be the most stable structure. The activated state for migration is the crowdion configuration, with an extremely low barrier ($\sim$0.01 eV), suggesting $1d$ (one-dimensional) diffusion at low temperatures and $3d$ diffusion at high temperature. In the case of Mo, the energy landscape between the ⟨111⟩ and ⟨110⟩ dumbbells is very shallow. Predicted migration energies and self-interstitial structures are consistent with experiment.

DOI: 10.1103/PhysRevB.66.220101 PACS number(s): 61.72.Ji, 71.15.Nc, 71.20.Be

Although self-interstitials are relatively rare in metals compared with vacancies under normal conditions, they are both plentiful and of prime importance in high-energy radiation environments[1] and in ion implantation.[2] For example, displacement cascades that form when high-energy neutrons impinge on metallic components of nuclear reactors produce large densities of vacancies and self-interstitials. The long time evolution of point defects into voids and clusters can embrittle these components and limit useful lifetimes.[3,4] Fusion reactor systems, under development, will be constructed of low-activation materials, such as vanadium alloys, ferritic steels or silicon carbide and the evolution of radiation damage in these materials is central to the feasibility of these systems.

Fundamental properties of self-interstitials in metals including the equilibrium structure and the migration barrier, are usually inferred from indirect measurements on irradiated samples.[5] However, the pairing or clustering of defects at high defect densities frequently obscures the interpretation of experimental data.[1] On the other hand, theoretical studies of self-interstitials have usually been performed using empirical potentials. Unfortunately, atomistic simulations based upon different empirical potentials yield widely disparate predictions for self-interstitials in body-centered cubic (bcc) metals.[6–8] While *ab initio* calculations can, in principle, alleviate this uncertainty, such calculations of interstitial properties have been very rare.[9] This is, in part, because atom-atom separations in the vicinity of interstitials are small compared with the equilibrium interatomic distance and very large simulation cells are required to account for the accompanying large relaxations.

In this communication, we report an extensive *ab initio* investigation of self-interstitials in bcc transition metals. We chose two representative elements for our study of self-interstitial structures, formation energies, and migration barriers: V for its aforementioned technological importance and Mo which is better characterized experimentally. Our results provide evidence for equilibrium interstitial configurations and migration mechanisms that are at variance with current understanding, but yet consistent with the extant experimental data. Additionally, our results provide experimentally inaccessible fundamental data required to fit empirical potentials appropriate for large-scale molecular dynamics simulation of radiation damage.

We adopt the ultrasoft pseudopotential formalism[10] based on density functional theory[11] and the GGA[12] for the exchange and correlation energies. One difficulty that we address is the highly compressed atomic bonding in the core region of the interstitial: bond lengths are shorter than in the bulk by as much as 15%. Such short distances between atoms can be correctly described by pseudopotentials with good transferability. The transferability is dictated, in large part, by whether semicore (SC) shells are frozen or determined variationally. Treating the SC shell as valence electrons guarantees the transferability to highly compressed systems[13] but also doubles the number of electrons to be explicitly described, thereby severely limiting the size of the supercell. We test the transferability of the pseudopotential without SC states by comparing the results with those calculated with SC pseudopotentials.

A cutoff energy of 30 Ry is used for the plane-wave basis to achieve convergence of the crystalline energy to within 0.05 eV/atom, except for the SC pseudopotential of V where 40 Ry is used to achieve the same level of convergence. The cold-smearing scheme[14] with a 0.2 eV width is used for broadening the density of states. In all calculations we relax the atomic positions until the Hellmann-Feynman forces are less than 5×10^{-2} eV/Å. In relaxing lattice vectors, damped cell dynamics[15] are used to ensure that each component of the stress tensor is less than 5×10^{-4} eV/Å^3. As a simple test, we compare the equilibrium lattice constant and the bulk modulus with the experimental values, as well as the results of all-electron calculations. As shown in Table I, the overall agreement is very good for both type of pseudopotentials although the SC pseudopotential is somewhat better.

To test the transferability of the pseudopotential without SC states to the low symmetry, short-bond situation (typical of split interstitials), we explicitly compare the self-interstitial formation energy (E_I^f) for the ⟨111⟩-dumbbell and ⟨110⟩-dumbbell configurations in Fig. 1 on $3\times3\times3$ simple-cubic supercells with both SC and non-SC pseudopotentials. The $E_I^f$is determined from

TABLE I. Comparison of the equilibrium lattice constant (a_0) and bulk modulus (B). The valence configurations are $(3s^2 3p^6)4s^2 4p^0 3d^3$ and $(4p^6)5s^1 5p^0 4d^5$ for V and Mo, respectively, with parenthesis indicating semicore (SC) states. The all-electron results are obtained with FLAPW and FP-LMTO method for V (Ref. 16) and Mo (Ref. 17), respectively.

	V		Mo	
	a_0(Å)	B(GPa)	a_0(Å)	B(GPa)
Pseudopotential (non-SC)	2.99	192	3.13	243
Pseudopotential (SC)	3.00	182	3.15	257
All electron (Refs. 16 and 17)	3.00	178	3.16	259
Expt. (Ref. 18)	3.02	160	3.15	260

$$E_I^f = E_{tot}(N+1) - \frac{N+1}{N} E_{tot}(N), \tag{1}$$

where $E_{tot}(N+1)$ and $E_{tot}(N)$ are the total energy of the system with and without a self-interstitial, respectively. For V, non-SC pseudopotential calculations predict formation energies which are 5–10% (0.2–0.3 eV) larger than those obtained with the SC pseudopotential. However, the magnitude of the overestimate is the same for both the $\langle 111 \rangle$ and $\langle 110 \rangle$ dumbbells, such that the non-SC pseudopotential can still be used to distinguish between competing interstitial configurations. On the other hand, formation energies computed with the non-SC pseudopotential for Mo are 20% (1.5–2.0 eV) below those obtained with the SC pseudopotential and the magnitude of the overestimates are not the same. The large differences between the formation energies obtained with and without SC states are associated with the very small interatomic separations within dumbbells. This is consistent with the well-known fact that the bond length of the Mo dimer is severely underestimated if the $4p$ semicore electrons are not explicitly included in the calculation.[19] In order to obtain more accurate results while overcoming the computational limitation, we introduce an approach where the SC pseudopotential is employed only for the interstitial atom and its neighbors [e.g., all of the atoms shown in Figs. 1(a) and 1(b)] and use the non-SC pseudopotential elsewhere. With this mixed-potential method, the error in the formation energy is now reduced to 5% while the relative differences are in agreement with purely SC potential results to within 0.05 eV. In the following calculations, we use the non-SC pseudopotential and the mixed-potential method for V and Mo, respectively.

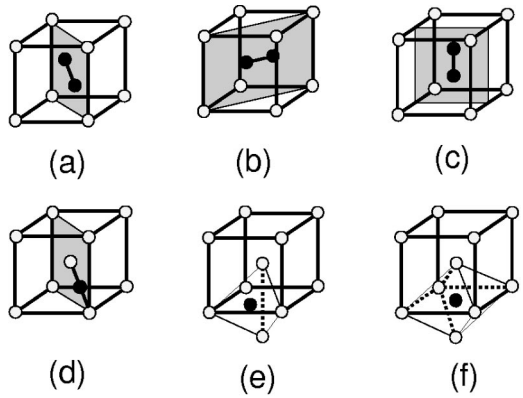

FIG. 1. Schematic pictures of interstitials studied here: (a) $\langle 111 \rangle$ dumbbell, (b) $\langle 110 \rangle$ dumbbell, (c) $\langle 100 \rangle$ dumbbell, (d) crowdion, (e) tetrahedral, and (f) octahedral.

Next, we test the convergence of E_I^f with respect to supercell size. We take a simple-cubic supercell and increase the size uniformly in each direction. In Table II, the convergence of E_I^f is shown for the $\langle 111 \rangle$ dumbbell in V. A supercell containing 250 atoms represents one of the largest systems ever studied in transition metals with *ab initio* methods. It can be seen that E_I^f converges to within 0.05 eV when a $4\times4\times4$ supercell with 129 atoms is used. Allowing the cell to relax significantly lowers E_I^f, resulting in an underestimate. This is because the actual strain around the interstitial in the infinite lattice lies between zero and the relaxed-cell value in these relatively small systems. A lower bound on the cell-relaxation energy is obtained from the fixed cell calculations as $E_{el} = V_0 P^2/2B$, where V_0 and P are the supercell volume and pressure, respectively. From Table II, we find that E_{el} can be used as a measure of the deviation of E_I^f(fixed cell) from its converged value for a given supercell size. Interestingly, the data reported in Table II converge with size faster than in empirical potential studies[9,20] where at least twice more atoms need to be included for a similar level of convergence. This is likely a consequence of electronic screening effects that are not adequately modeled by empirical potentials.

The convergence behavior of E_I^f is similar for the other interstitial configurations in V. In the case of Mo, the error from the convergence profile is about 0.1 eV for the $4\times4\times4$ supercell, in agreement with the estimate obtained using

TABLE II. Convergence of E_I^f for $\langle 111 \rangle$ dumbbell of V with respect to the supercell size. $E_I^f(1)$ and $E_I^f(2)$ indicate the formation energy for the fixed and relaxed cells, respectively. $N_{\mathbf{k}}$ is the number of **k**-points sampled in the first Brillouin zone. The energy and pressure (P) are in eV and GPa, respectively. The pressure is one third of the trace of the stress tensor for the fixed cell.

Supercell	N_{atom}	$N_{\mathbf{k}}$	$E_I^f(1)$	P	E_{el}	$E_I^f(2)$
$(2a_0)^3$	16(+1)	64	4.49	17.3	0.80	3.46
$(3a_0)^3$	54(+1)	27	3.28	4.6	0.23	2.99
$(4a_0)^3$	128(+1)	8	3.14	1.4	0.06	3.10
$(5a_0)^3$	250(+1)	8	3.12	0.5	0.01	3.06

TABLE III. The formation energies of various interstitials in 4×4×4 supercells with a fixed volume. Energies are in eV.

	⟨111⟩	⟨110⟩	⟨100⟩	Crowdion	Tetrahedral	Octahedral
V	3.14	3.48	3.57	3.15	3.69	3.62
Mo	7.34	7.51	8.77	7.34	8.20	8.86

E_{el}. Since the 5×5×5 supercell is too large for routine calculations,the E_I^f results reported below are all obtained using the 4×4×4 supercell at fixed volume, except as noted.

Table III shows the full set of E_I^f for V and Mo. Either the ⟨111⟩ dumbbell or the crowdion is the most stable configuration in both metals. The small difference, less than 0.01 eV between the ⟨111⟩ dumbbell and the crowdion, is well below the intrinsic accuracy of our density functional calculations. The difference between the ⟨111⟩ and ⟨110⟩ dumbbells in Mo is nearly twice as large as our estimated convergence error with a 4×4×4 supercell. However, to insure that the ⟨111⟩ dumbbell is the most stable interstitial configuration in Mo, additional calculations are performed using a 5×5×5 supercell. In this case, the energy difference between the ⟨111⟩ and ⟨110⟩ dumbbells is 0.23 eV (rather than 0.17 eV), confirming that the ⟨111⟩ dumbbell is the most stable interstitial in Mo.

The prediction that the ⟨111⟩ dumbbell is the most stable interstitial configuration is at variance with the widely accepted view that the ⟨110⟩-dumbbell is the equilibrium interstitial in bcc metals[1,6–8,20]. Previous calculations, however, were based upon embedded-atom-method (EAM) potentials fitted to reproduce equilibrium bulk properties. For V, our calculated formation energy (3.14 eV) is well below the values from previous EAM calculations (4.61–4.78 eV).

The systematic discrepancy with EAM results arises from the fact that those formation energies are dominated by the short-range pair potential. The overestimation of E_I^f arises because EAM parametrizations typically fit the isotropically compressed equation of state.[21] This fit is done by adjusting the pairwise potential, but actually captures two effects, the pairwise ion-ion repulsion and the volume dependent kinetic energy of the electrons. Thus the actual pairwise repulsion is overestimated; rising too steeply at small separations. For the interstitial, whose formation is accompanied by significantly shorter interatomic distances but by only a small reduction in volume, the EAM pairwise repulsion is too strong and E_I^f is consequently too high.

In order to understand the underlying physics determining E_I^f, we inspect atomic relaxations for each dumbbell. The strain field surrounding the dumbbell closely resembles a uniaxial strain along the symmetry direction of the dumbbell. This suggests that the modulus associated with the uniaxial strain in the direction of the dumbbell, $M_{[ijk]}$, will be correlated with E_I^f. As shown in Table IV, the magnitudes of the $M_{[ijk]}$'s are exactly in the same order as the E_I^f for the ⟨ijk⟩ dumbbells. It is somewhat surprising that $M_{[111]}$ is the smallest modulus, in spite of the fact that the nearest-neighbor interatomic bonds point in this direction. This is possible because the number of approaching neighbors is only two, compared to four and eight for ⟨110⟩ and ⟨100⟩ dumbbells, respectively. While this approach describes bcc V and Mo, it predicts that the ⟨100⟩ interstitial is most stable for Fe, in disagreement with *ab initio* results.[9] It is interesting to note that while the ratio of the Mo and V cohesive energies is 1.3, the ratio of the E_I^f is 2.3 on average. This extraordinary difference violates the rule of thumb that defect formation energies scale as the cohesive energy. However, much of the formation energies of self-interstitial dumbbells is associated with strain energy, hence the ratio of the $M_{[111]}$'s should be a better predictor. This is born out by the data in Table IV .

TABLE IV. Theoretical values for the modulus associated with uniaxial strain, $M_{[111]}=(C_{11}+2C_{12}+4C_{44})/3$, $M_{[110]}=(C_{11}+C_{12})/2+C_{44}$, and $M_{[100]}=C_{11}$, where C_{11}, C_{12}, and C_{44} are elastic constants of the simple cubic cell. Units are GPa.

	$M_{[111]}$	$M_{[110]}$	$M_{[100]}$
V	221	234	271
Mo	395	410	454

To estimate the migration barrier of self-interstitials, we investigate the diffusion of the ⟨111⟩ dumbbell to neighboring sites along the same ⟨111⟩ direction. We find that the crowdion is the transition state along the diffusion path and the diffusion barrier is simply the difference of E_I^f between the ⟨111⟩ dumbbell and the crowdion. As shown in Table III, this energy is very small (~0.01 eV), which is consistent with the anomalously high diffusivity of the self-interstitial found in experiments on V even at very low temperatures.[22] Even though the maximum atomic displacement required to reach the saddle configuration is not small (~0.2 Å), the change in the actual bond lengths is minor, producing only very small changes in the electronic density of states and energy. This extremely low activation energy for migration in the ⟨111⟩ direction suggests a picture in which the dynamics of self-interstitial diffusion should not be normal Brownian motion on the lattice but rather a Levy flight (although on

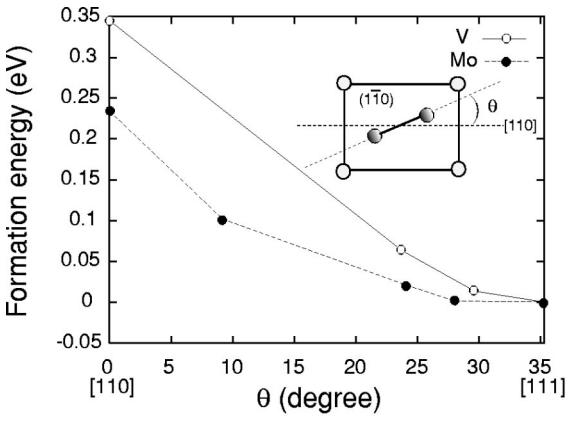

FIG. 2. The formation energy of the interstitials with orientations between [111] and [110] relative to that for the ⟨111⟩ dumbbell. $\theta=0°$ and $\theta=\tan^{-1}(1/\sqrt{2})\simeq 35.3°$ correspond to the [110] and [111] directions, respectively.

the lattice), where the interstitials move a random distance along a particular ⟨111⟩ direction followed by thermally excited crowdion reorientation to another ⟨111⟩ direction.

Self-interstitial diffusion in Mo has received more experimental attention than V. We find that the ⟨111⟩ dumbbell migration energy in Mo is 0 to within the uncertainty of the present calculations (± 0.05 eV), in agreement with experimental measurements (0.05 eV).[1] On the other hand, the ⟨111⟩-dumbbell orientation found here is apparently inconsistent with the diffuse x-ray scattering experiment, which shows the ⟨110⟩-dumbbell configuration with the orthorhombic displacement field is in agreement with the data rather than the ⟨111⟩ dumbbell with the trigonal symmetry.[1,23] The origin of this discrepancy could be associated with the approximate description of the exchange-correlation energy within the GGA framework. To investigate this possibility, we repeated the calculation of the ⟨111⟩ and ⟨110⟩ dumbbells in Mo within the LDA framework. In this case, we find that the ⟨111⟩ dumbbell is more stable than the ⟨110⟩-dumbbell by 0.15 eV, which is very close to the 0.16 eV value found using GGA (Table III). This suggests that the relative stability of these two interstitials is insensitive to the form of the exchange-correlation energy used.

It is also possible that the dumbbell orientation in Mo is neither ⟨111⟩ nor ⟨110⟩, but rather lies somewhere between these. The E_I^f versus dumbbell orientation is shown in Fig. 2 for both V and Mo (the Mo results are obtained using an $5\times5\times5$ supercell). While the ⟨111⟩ dumbbell is clearly stable in V, the E_I^f versus dumbbell orientation curve in Mo is extremely shallow near the ⟨111⟩ orientation. This implies that a ⟨111⟩ dumbbell would thermally wobble with a large amplitude even at low temperatures. Such a thermal motion will substantially perturb the trigonal symmetry in the long-range displacement field of a ⟨111⟩ dumbbell and produce a diffraction pattern as shown in Ref. 23. The shallow energy surface for Mo also suggests that even very small stresses within a sample would produce substantial canting of the dumbbell away from ⟨111⟩ . Such a stable canted dumbbell is also compatible with the diffuse x-ray results since it has a lower symmetry than a ⟨111⟩ dumbbell.[23]

We thank B. Wirth, S. Dudarev, A. Sutton, D. Pettifor, and K. Burke for helpful discussions. The PWSCF package[24] was used in this study and computations were performed at NERSC and the Keck Materials Science Computing Center at Princeton University. S.H. was partially supported by KOSEF. This work was supported by US DOE Grant No. DE-FG02-01ER54628 and LLNL.

[1] F.W. Young, Jr., J. Nucl. Mater. **69/70**, 310 (1978).
[2] K. Nordlund *et al.*, Nature (London) **398**, 49 (1999).
[3] T. Diaz de la Rubia *et al.*, Nature (London) **406**, 871 (2000).
[4] E.E. Bloom, J. Nucl. Mater. **258-263**, 7 (1998).
[5] *Fundamental Aspects of Radiation Damage in Metals*, edited by M. T. Robinson and F. W. Young Jr., ERDA report Conf 751006 NT 15 (Springfield, Virginia, 1976).
[6] G. Simonelli, R. Pasianot, and E.J. Savino, Phys. Status Solidi B **217**, 747 (2000).
[7] J.B. Adams and S.M. Foiles, Phys. Rev. B **41**, 3316 (1990).
[8] J.M. Harder and D.J. Bacon, Philos. Mag. A **54**, 651 (1986); G.J. Ackland and R. Thetford, *ibid.* **56**, 15 (1987).
[9] C. Domain and C.S. Becquart, Phys. Rev. B **65**, 024103 (2001).
[10] D. Vanderbilt, Phys. Rev. B **41**, 7892 (1990).
[11] P. Hohenberg and W. Kohn, Phys. Rev. **136**, B864 (1964).
[12] J.P. Perdew, K. Burke, and M. Ernzerhof, Phys. Rev. Lett. **77**, 3865 (1996).
[13] A. Laio *et al.*, Science **287**, 1027 (2000).
[14] N. Marzari *et al.*, Phys. Rev. Lett. **82**, 3296 (1999).
[15] R.M. Wentzcovitch, Phys. Rev. B **44**, 2358 (1991).
[16] WIEN97 code was used with the GGA functional.
[17] T. Korhonen, M.J. Puska, and R.M. Nieminen, Phys. Rev. B **51**, 9526 (1995).
[18] *Handbook of Chemistry and Physics*, 81st ed. (CRC Press, Ohio, 2000-2001).
[19] J. Bernholc and N.A.W. Holzwarth, Phys. Rev. Lett. **50**, 1451 (1983).
[20] W. Xu and J.A. Moriarty, Phys. Rev. B **54**, 6941 (1996).
[21] J.H. Rose *et al.*, Phys. Rev. B **29**, 2963 (1984).
[22] R.R. Coltman *et al.*, Radiat. Eff. **24**, 69 (1975).
[23] P. Ehrhart, J. Nucl. Mater. **69**, 200 (1978).
[24] S. Baroni *et al.*, http://www.pwscf.org